12th International Conference on Nuclear Engineering
April 25-29, 2004, Arlington, Virginia USA

ICONE12-49151

A TECHNIQUE FOR DYNAMIC CORROSION TESTING IN SUPERCRITICAL CO2

Eric P. Loewen
Bechtel BWXT Idaho, LLC
Idaho National Engineering and Environmental Laboratory
P.O. Box 1625
Idaho Falls, Idaho 83415-3860
USA
(208) 526-9404
(208) 526-2930 (fax)
loewep@inel.gov

Cliff B. Davis
Bechtel BWXT Idaho, LLC
Idaho National Engineering and Environmental Laboratory
P.O. Box 1625
Idaho Falls, Idaho 83415-3890
USA
(208) 526-9470
(208) 526-6971 (fax)
cbd@inel.gov

David E. Shropshire
Bechtel BWXT Idaho, LLC
Idaho National Engineering and Environmental Laboratory
P.O. Box 1625
Idaho Falls, Idaho 83415-3870
USA
(208) 526-6800
des@inel.gov

Kevan Weaver
Bechtel BWXT Idaho, LLC
Idaho National Engineering and Environmental Laboratory
P.O. Box 1625
Idaho Falls, Idaho 83415-3870
USA
(208) 526-0321
weavkd@inel.gov

Keywords: Carbon Dioxide, Supercritical CO_2, Corrosion, ATHENA, Fast Reactor

ABSTRACT

An experimental apparatus for the investigation of the flow-assisted corrosion of potential fuel cladding and structural materials to be used on a fast reactor cooled by supercritical carbon dioxide has been designed. This experimental project is part of a larger research at the Department of Energy being lead by the Idaho National Engineering and Environmental Laboratory (INEEL) to investigate the suitability of supercritical carbon dioxide for cooling a fast reactor designed to produce low-cost electricity as well as for actinide burning.

The INEEL once-through corrosion apparatus consists of two syringe pumps, a pre heat furnace, a 1.3 meter long heated corrosion test section, and a gas measuring system. The gas flow rates, heat input, and operating pressure can be adjusted so that a controlled coolant flow rate, temperature, and oxygen potential are created within each of six test sections. The corrosion cell will test tubing that is commercially available in the U. S. and specialty coupons to temperatures up to 600°C and a pressure of 20MPa.

The ATHENA computer code was used to estimate the fluid conditions in each of the six test sections during normal operation.

INTRODUCTION

This experimental project is part of a larger Fast Gas Reactor research at the INEEL to investigate the suitability of a fast reactor cooled by supercritical carbon dioxide for producing low-cost electricity as well as for actinide burning. The goal is to identify and analyze the key technical issues in core neutronics, materials, thermal-hydraulics, fuels, and economics associated with the development of this reactor concept. This paper is focused on the project's efforts in material testing; specifically corrosion tests at high temperature and pressure.

Gas cooled reactors have a long history that date back to the very early days of nuclear energy development. Most of the early development centered on low temperature systems using a graphite moderator, metal clad metallic fuel, and carbon dioxide as a coolant. Commercial deployment of such systems started in the mid-1950's, primarily in the United Kingdom and France, with the natural uranium fueled Magnox stations, followed by higher temperature, low enriched uranium fueled advanced gas cooled reactor stations, solely deployed in the United Kingdom, starting in the mid-1970's. Although these two pioneering programs have now concluded, experience from the over 1,000 reactor-years of operation provides the stepping stone for the Generation IV gas reactors operating at higher temperature and pressures.

There have been a total of 52 electricity generating, carbon dioxide cooled reactor plants placed in operation worldwide. The British were early pioneers in the field of gas-cooled reactors and made significant contributions to high-temperature gas reactor development, especially in the areas of fuel, core and heat transfer technology. The first gas-cooled reactor was constructed in 1962; and an extensive program was undertaken to build twenty-five more Magnox reactors for electricity production. These reactors are fueled with natural uranium metal, clad with Magnox (a magnesium-aluminum alloy), and use CO_2 as the coolant. The early Magnox plants had steel pressure vessels while the later, higher output versions used prestressed concrete reactor vessels. However, the higher power output versions had to be derated by approximately 20% following the discovery of a steel oxidation problem in 1969. Fourteen Advanced Gas Reactor were placed in service after the Magnox deployment becoming the mainstay of the British nuclear reactor program. These advanced reactors had higher energy output and on-line refueling.

The French developed a version of Magnox reactors in the 1960s using both an external CO_2 system and an "integral' system, where the main CO_2 system is included inside the pressure vessel. Although, their eight-prototype Magnox gas cooled reactors performed well, because of their high operating costs compared to the pressurized water reactors in France, the reactors were eventually shut down.

Japan built a single, small (160 MWe) demonstration gas cooled Magnox plant, Tokai-1, in the 1960s. Recognizing the industrial need for high temperature heat, 35% of the reactor output is used to provide heat between 300°C and 900°C. For example coal gasification and thermochemical water splitting require process heat at temperatures of 900°C or higher.

Relative to the material compatibility issues, it was found that when steel is exposed to carbon dioxide at temperatures in the range of 350°C to 450°C, a thin protective coating of magnetite (Fe_3O_4) is formed. This coating thickens at a slow rate and ultimately cracks whereupon local pits and excrescences form, permitting more rapid oxidation.

At the design stage the evidence suggested that oxidation rates were moderate on exposed surfaces. The first gas-cooled reactors were, therefore, constructed from mild steel and the use of the more expensive stainless steel was restricted to essential applications for plant economics considerations. However, reactor research program identified problems involving the corrosion and oxidation of the components made from Magnox alloy (a magnesium-aluminum alloy), and of the steel shell when wet CO_2 conditions existed. The oxidation effects from CO_2 samples tested at 400°C, 0.8 MPa, and varying moisture contents, are shown in Table 1 (Nucleonics, 1956).

Table 1: Oxidation of materials in CO_2 at 400°C and 0.8MPa.

Material	Oxidation
18/8/1 stainless steel, Commercial A1 Sintered A1 powder	*Excellent* (no attack after 5 months)
Pure Mg ***Magnox C*** Mg alloy AM503 AL alloy RR58	*Good* (0.1 mg/ cm^2 / 5 months)
Al alloy RR57 Mg alloy ZT1 Mg alloy ZRE1 Magnox E Alloy steel (Jessops G1) Mild steel (0.05% C) Sintered Mg powder Pressure-vessel steel	*Moderate* (0.15 – 1.11 mg/ cm^2/ 5 months)
Cast iron	*Poor* (2.72 mg/cm^2 / 5 months)

The overall objectives of this current research are to:

1) Deploy a corrosion test apparatus at the INEEL to carry out an independent investigation of the corrosion of potential fuel cladding and reactor structural materials exposed to high-temperature, supercritical CO_2.
2) Develop techniques to quantify the corrosion rate of metals exposed to supercritical CO_2.
3) Obtain corrosion data on different metals exposed to supercritical CO_2.
4) Systematically understand the addition of silicon in the formation of protective layers on steel surfaces.

DESIGN

An experimental unit is being built at INEEL to test corrosion in an environment that approaches the conditions that would be present in a fast gas reactor. The oxide layer on the metal components will be controlled in the belief that it will provide a protective coating, thereby limiting corrosion.

An overall diagram of the experimental apparatus is provided in Fig. 1. A tube furnace controlled by K-type thermocouples provides the heated zone for the six independent test sections. Process gas is supplied from standard high-

pressure CO_2 gas bottles using a liquid withdrawal. Venting of the experimental system will be through a letdown throttle valve for post-test gas sampling. Each major experimental sub-system is described below:

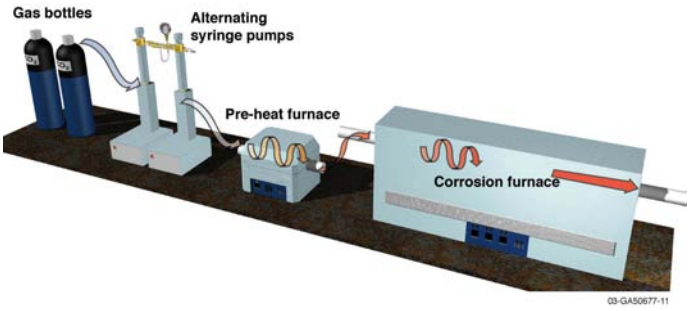

Fig. 1. Experimental apparatus.

1) Gas Supply System: Two pressure-regulated manifolds will deliver 99.9999% CO_2 to the suction of the syringe pumps. The CO_2 gas stream can be augmented with different gases such as Ar, CO, CH_4, H_2O, or N_2 to better simulate the radiolytic decomposition of gases under a neutron flux.
2) Pressure Supply: Two ISCO Series D syringe pumps will take the liquid CO_2 at room temperature and 5.5MPa to a maximum pressure of 21MPa. The pumps have a flow rate range of 1 to 25ml/min.
3) Preheater Furnace: The preheater furnace is a Lindberg Model 55030-B-COM and has a maximum operating temperature of 1100°C. The single zone split hinge tube furnace is 60cm long with a 2.54cm diameter alumina tube. The coolant is contained within a flow tube that passes through the alumina tube. The maximum power of the heater is 8 kW, which will take the high-pressure gas stream and increase the temperature to 300°C before entering the corrosion furnace.
4) Corrosion Furnace: The tube furnace is a Lindberg Model 55666-B-COM with a maximum operating temperature of 1100°C. The internal diameter of the tube furnace, lined with an alumina tube, is 10cm accommodating six different flow tubes with outer diameters up to 1.30cm. The furnace has a heated length of 1.3m with three separate heating zones that are controlled by three separate Yokogawa UP150 programmable controllers. The length allows the establishment of fully-developed, steady flow conditions. The maximum power output is 11 kW.
5) Filtering: The CO_2 passes through inline filters (0.5μm) upstream and downstream of the furnace. The differential pressure across the filter is monitored during the experiment for the early detection of breakaway corrosion in the test section.
6) Gas Sampling: The CO_2 is rejoined into one gas line downstream of the furnace and routed to the pressure letdown valve. The low pressure CO_2 will then be directed to the gas sampling system that uses a mass spectrometer, an O_2 meter, and a CO/CO_2 meter.

Table 2 presents a summary of the planned experimental parameters. The temperature and pressure values closely match the current design case. The experimental duration is limited to 1,000 hours to obtain initial corrosion data, but obviously needs validation at longer exposure times (i.e. 3,000 hours).

Table 2. Proposed experimental test matrix.

Metal	Temperature (ºC)	Time (Hours)	P (MPa)
Fe, Fe-Si	450-600	1,000	15-20
Austenitic steels	450-600	1,000	15-20
Ferritic steels	450-600	1,000	15-20
Titanium	450-600	1,000	15-20
OSD Materials	450-600	1,000	15-20

ATHENA MODEL

The ATHENA computer code (Carlson et al., 1986) was used to simulate the corrosion experiment. The ATHENA code is incorporated as a compile time option in the RELAP5-3D computer code (the RELAP5-3D Development Team, 2002. The principal difference between RELAP5 and ATHENA is that RELAP5 was designed to use water as the working fluid while ATHENA allows the use of many different working fluids, including supercritical CO_2. ATHENA was modified to use the Jackson (2002) forced convection correlation for this analysis. The Jackson correlation was developed for forced convection heat transfer from tubes to supercritical water and carbon dioxide. The code also evaluated the heat transfer coefficient for fully developed laminar flow and used the maximum of the values from the forced convection and laminar correlations.

An ATHENA input model of the corrosion experiment was developed as illustrated in Fig. 2. The model represents the portion of the experimental apparatus between the CO_2 supply bottles and the letdown valve. The CO_2 bottles were modeled as a time-dependent volume (Component 100) containing saturated liquid at 18°C. The syringe pumps (Component 135) were modeled as a time-dependent junction. The flow rate was set at 25ml/min, which corresponds to the maximum value delivered by the pumps.

The preheater (Component 150) was modeled as a 1.57-cm inner diameter tube containing ten control volumes and heat structures. The 2.54-cm diameter alumina tube was not modeled explicitly. Instead, the outer wall temperature of the 1.57-cm diameter flow tube was varied to obtain an exit fluid temperature of 300°C. The furnace was modeled with six parallel pipes (Components 176, 186, 206, 216, 236, and 246) corresponding to the six flow tubes in the experiment. The inner diameters of the flow tubes are 0.175cm (Components 176 and 186), 0.457cm (Components 206 and 216), and 1.02

cm (Components 236 and 246). The outer walls of the flow tube heat structures were set at 600°C. Heat structures were used to compute the heat loss to the environment from the un-insulated tubes downstream of the furnace. The heat loss accounted for natural convection and radiation from the tubes to the environment.

The hydraulic resistance of the filters was modeled with a large form loss coefficient (140 based on the area of the adjacent tube). The six lines between the inlet cross (Component 170) and the outlet header (Component 260) are identical except for the losses associated with the diameter of the heated flow tube and the losses at the inlet cross and outlet header. The area of the letdown valve (Component 275) was adjusted to control the pressure in the test section at 20.8MPa. The pressure downstream of the letdown valve was set at atmospheric pressure using a time-dependent volume (Component 310).

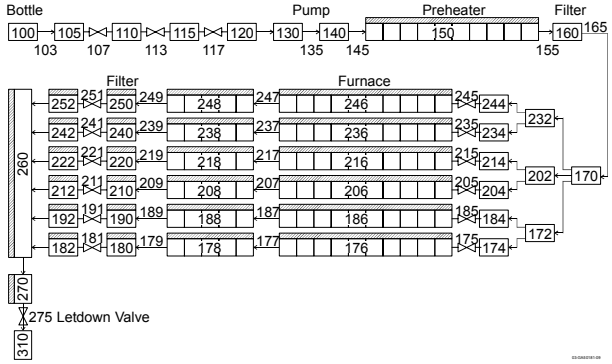

Fig. 2. Nodalization of the ATHENA input model.

RESULTS

The ATHENA model illustrated in Fig. 2 was used to calculate the thermal-hydraulic conditions in the test section at the maximum flow rate. The results of the steady-state calculation are shown in Table 3. The work done by the syringe pumps raises the fluid temperature at the inlet to the preheater above the ambient temperature. The preheater and furnace then raise the fluid temperature to 300°C and 600°C, respectively. The fluid temperature at the exit of the preheater is more than 400°C below the outer wall temperature of the flow tube whereas the fluid temperatures at the exit of the furnace nearly equal the outer wall temperature. The longer length of the furnace and the division of the flow between six parallel channels increase the residence time of the fluid in the test section and allow it to more closely approach the wall temperature compared to the preheater, which is relatively short and experiences the combined flow. The heat loss from the un-insulated tubes downstream of the test section is significant. The temperature at the letdown valve is more than 300°C below the temperature at the outlet of the furnace.

Table 3. Steady-state conditions at maximum flow rate.

Parameter	Value
Pressure, MPa	20.8
Mass flow rate, kg/s	6.52e-4
Preheater inlet temperature, °C	36.3
Preheater exit temperature, °C	300.0
Preheater outer wall temperature, °C	753.1
Furnace outer wall temperature, °C	600.0
Furnace exit temperature, °C	599.0 - 600.0
Letdown temperature, °C	87.8
Preheater power, kW	0.30
Furnace power, kW	0.24
Heat loss, kW	0.46
Differential pressure, kPa	0.96

Fig. 3 shows the calculated fluid temperature in the flow tubes as a function of normalized length through the furnace. The fluid temperature in each flow tube rapidly approached the imposed wall temperature. The temperature initially increased more rapidly in the smaller tubes, but the temperature was nearly uniform at the exit of the furnace.

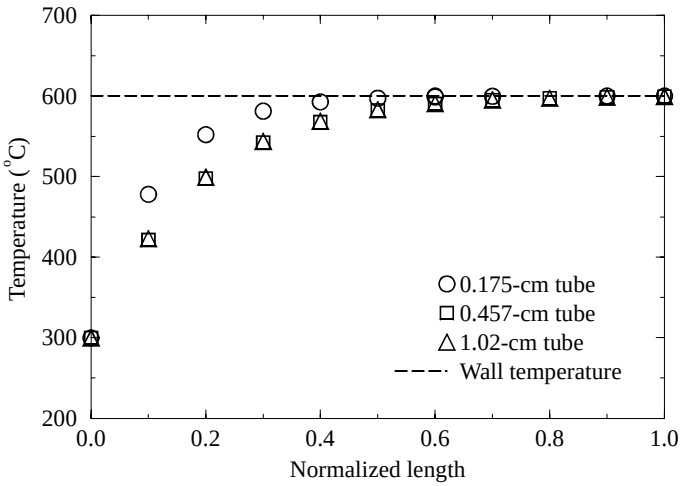

Fig. 3. Fluid temperature in the flow tubes as a function of normalized length.

Fig. 4 shows the calculated Reynolds number as a function of normalized length through the furnace. The average Reynolds number was about 2000 in the 0.175-cm diameter tube, 860 in the 0.457-cm diameter tube, and 380 in the 1.02-cm tube. The variation in Reynolds number with respect to length was less than 15%. Since the maximum flow rate from the syringe pumps was used in this calculation, Fig. 4 indicates that the test section will primarily experience laminar flow during the corrosion tests.

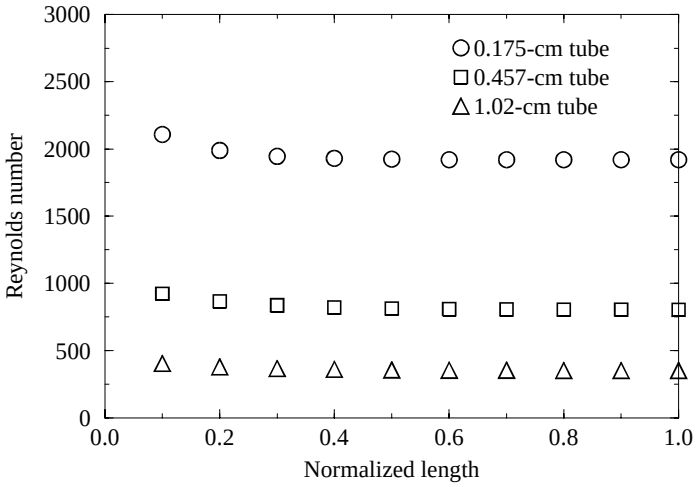

Fig. 4 Reynolds number in the flow tubes as a function of normalized length.

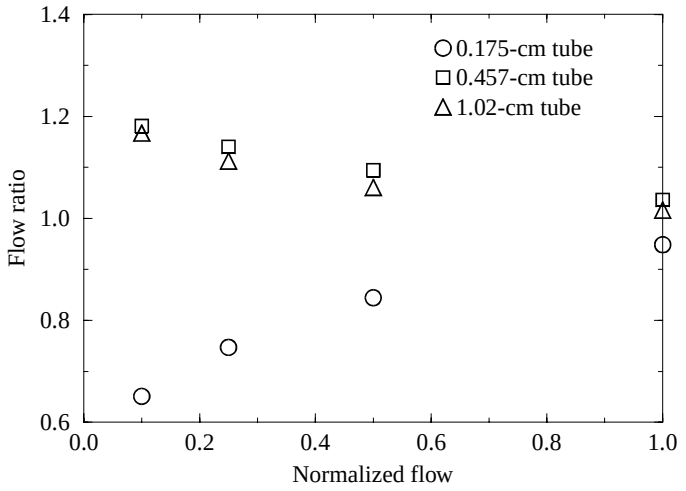

Fig. 5 Flow ratio for each flow tube diameter as a function of normalized flow.

Several calculations were performed to determine the flow split through the test section as a function of total flow rate. Fig. 5 shows the ratio of the flow through each tube to the average flow through six flow tubes as a function of normalized flow rate. A ratio of unity corresponds to an equal mass flow rate through all six tubes. At a normalized flow rate of unity, which corresponds to the maximum system flow as described in Table 3, the six flow tubes receive nearly the same mass flow. The flow rate through the smallest tube is within 5% of the average value. Even though the hydraulic resistance of the smallest tube is much larger than that of the largest tube (its flow area is more than 30 times smaller), the overall hydraulic resistance in each line is nearly the same at the maximum flow because the filter dominates the resistance. However, as the normalized flow rate decreases, the laminar friction factor increases and the relative significance of the resistance due to the tube length in the furnace increases. At a normalized flow rate of 0.10, the flow through the smallest tube is 65% of the average value. The results shown in Fig. 5 were obtained assuming that the form loss coefficient associated with the filter remains constant. Although data from the manufacturer are not available in the range of interest here, the available data shows that the form loss coefficient increases as the flow rate decreases. If this trend continues as the flow rate decreases to the range of interest here, the results presented in Fig. 5 should bound the actual variation in flow between tubes. Fig. 5 also shows that the flow through the 0.457-cm tubes is slightly higher than the flow through the 1.02-cm tubes. This unexpected result is caused by larger form loss coefficients at the inlet cross and the exit header for the larger tube.

CONCLUSIONS

The INEEL is developing an experiment to study the effects of temperature, flow, gas composition, and oxidation potential on the corrosion characteristics of typical structural materials that could be used in a gas cooled fast reactor with CO_2 coolant.

ATHENA calculations were performed to determine fluid states in the test section during normal operating conditions. The calculations showed that the fluid temperature in the flow tubes is nearly uniform at the exit of the furnace. The calculations also showed that the flow in the test section is laminar even at the maximum system flow rate. The flow is almost uniformly divided between the six tubes at the maximum flow rate. The flow split becomes less uniform as the total flow rate is decreased. At a flow rate corresponding to 10% of the maximum value, the flow through the smallest tube is about 65% of the average value.

Future ICONE publications will provide experimental results.

ACKNOWLEDGMENT

Work supported through the INEEL Long-Term Research Initiative Program under DOE Idaho Operations Office Contract DE-AC07-99ID13727.

REFERENCES

"Calder Hall", A Special Report, Nucleonics, Vol. 14, No. 12, Dec. 1956.

Agnew, H.M., 1981: "Gas-Cooled Nuclear Power Reactors," Scientific American, vol. 244, no. 6, June, pp. 55-63.

Taylor, G.M., 1989a: "Hunterston A and B: Operating the Magnox and AGR," Nuclear News, vol. 32, no. 5, April, pp.52-67.

Carlson, K. E., Roth, P. A., and Ransom, V. H., 1986, "ATHENA Code Manual Vol. I: Code Structure, System Models, and Solution Methods," Idaho National Engineering Laboratory, EGG-RTH-7397.

Jackson, J. D., 2002, "Consideration of the Heat Transfer Properties of Supercritical Pressure Water in Connection with the Cooling of Advanced Nuclear Reactors," *Proceedings of the 13th Pacific Basin Nuclear Conference*, Shenzhen, China, 21-25 October.

The RELAP5-3D© Development Team, 2002, "RELAP5-3D Code Manual," Idaho National Engineering and Environmental Laboratory, INEEL-EXT-98-00834, Revision 2, July.